International Journal of Control, Automation and Systems 19(4) (2021) 1539-1549
http://dx.doi.org/10.1007/s12555-020-0255-6
ISSN:1598-6446 eISSN:2005-4092
http://www.springer.com/12555

Adaptive Nonsingular Integral-type Second Order Terminal Sliding Mode Tracking Controller for Uncertain Nonlinear Systems

Saleh Mobayen*, Hamede Karami, and Afef Fekih

Abstract: Achieving accurate and reliable tracking control for nonlinear systems with uncertainties and disturbances is one of the most challenging problems in nonlinear control. In this paper, we propose an adaptive nonsingular integral-type second order terminal sliding mode tracking control for nonlinear systems with uncertainties. First an integral type sliding manifold is defined to ensure finite time tracking convergence. Then an adaptation mechanism is proposed to estimate the unknown uncertainty upper bound. Finally, the adaptive nonsingular integral-type second order terminal sliding mode controller is synthesized without any assumptions about the uncertainties. System stability is proven using the Lyapunov stability theorem. Its performance is assessed using a thruster system and an inverted pendulum. Chattering attenuation, finite time convergence and disturbance mitigation are among the positive features of the proposed approach. Additionally, eliminating the need for the upper bound knowledge resulted in a design that can practically be implemented to a wide range of applications.

Keywords: Adaptive nonsingular control, nonlinear system, second order sliding mode, terminal sliding mode, tracking control.

1. INTRODUCTION

1.1. Background and motivation

Trajectory tracking or stabilization of nonlinear systems with uncertainties is an important topic in mechanics, robotics, medicine, control of electromechanical systems, etc [1, 2]. Hence, much attention has been given to this topic in the last decades [3–7]. Among the numerous nonlinear control methods, Sliding Mode Control (SMC) has gained special interest [8–11]. Robustness to uncertainties and parameter variations, fast dynamic response, and ease of implementation are among its attractive features [12–14]. However, the chattering phenomenon, i.e., high frequency finite amplitude oscillations, is the main drawback of this methodology, which can damage mechanical systems and lead to degradation of tracking performance and robustness. Substituting the sign function by some other softened approximation such as hyperbolic tangent and saturation can alleviate the chattering effects in some systems [15, 16]; however, this may reduce the system's robustness [17]. The use of smoothing devices and rigid body assumptions are other methods employed to counteract chattering; nevertheless, they are not executable for all control input frequencies [18]. Another approach is online disturbance estimation [19, 20]; but, its accuracy depends on the sampling step. High Order Sliding Mode Control (HOSMC) was shown to significantly reduce the chattering effects [21–23]. A special type of HOSMC is the Second Order Sliding Mode Control (SOSMC). This methodology is based on the usage of a sign function on the time derivative of the control law [24]. Using integration, the control input is obtained and the chattering problem is reduced [24, 25]. The SOSMC has several superiorities than conventional SMC such as finite time stability, extension of the relative degree of sliding variable in SMC, reduction of chattering and increase the accuracy of close-loop system [26–28].

1.2. Literature review

In [29], the classic sliding mode control and SOSMC were compared in terms of the chattering phenomena effects. It showed that increasing the un-modeled dynamics resulted in an increase in the chattering amplitude in conventional SMC control and the super-twisting algorithm. Therefore, if disturbance value increases, the conventional control is more efficient and the un-modeled dynamic bound and disturbance value should be considered for the

Manuscript received April 11, 2020; revised July 2, 2020; accepted July 22, 2020. Recommended by Associate Editor DaeEun Kim under the direction of Editor Hamid Reza Karimi.

Saleh Mobayen is with the Department of Electrical Engineering, Faculty of Engineering, University of Zanjan, Zanjan, Iran and Future Technology Research Center, National Yunlin University of Science and Technology, 123 University Road, Section 3, Douliou, Yunlin 64002, Taiwan, R.O.C. (e-mail: mobayen@znu.ac.ir; mobayens@yuntech.edu.tw). Hamede Karami is with the Department of Electrical Engineering, Faculty of Engineering, University of Zanjan, Zanjan, Iran (e-mail: hamede.karami@gmail.com). Afef Fekih is with the Department of Electrical and Computer Engineering, University of Louisiana at Lafayette, Lafayette, USA (e-mail: afef.fekih@louisiana.edu).
* Corresponding author.

chattering control. However, these results have not been validated by other approaches such as disturbance estimation and smooth function, and for some systems this comparison may not be extensible. In [30], the time speci?ed Terminal Sliding Mode Control (TSMC) is provided for robotic airship's trajectory tracking. Though this method could specify the finite time convergence, it did not eliminate chattering and one of the switching surfaces could not converge to the origin. The SOSMC for nonlinear affine systems with quantized uncertainty based on non-smooth switching line was presented in [31]. However, the uncertainty was assumed to be known and the chattering effects were not eliminated. In [32], four control strategies were designed to adjust the control law's amplitude. Though the adaptive SOSMC strategies were shown to achieve the control objectives in the presence of disturbances and parameter variations, the chattering and perturbation effects have not been eliminated. In [33], an SOSMC is designed for systems with output constraints; however, the uncertainty bounds were assumed to be known. Furthermore, the chattering problem was obvious and an increase in the initial values of states prevented the sliding surface and its derivative from converging to the origin. In [34], an adaptive discrete SOSMC method was proposed to decrease data sampling inaccuracy and uncertainty of the system models. Its implementation to the tracking control of a combustion engine showed that that the second order discrete sliding mode control improves the performance compared to a classic discrete SMC with sampling inaccuracy and uncertainty. In [35], a mixture of switched policy and time-based adaptation for SOSMC is presented. In this approach, the control law is adjusted using the uncertainty's actual size. The controller is synthesized based on the assumption that the uncertainty's upper bound is known and the state-space system is partitioned. In each partition, the upper and lower bounds of the uncertainty are defined. As a result, the chattering effect cannot be eliminated. In order to obtain a more realistic design, it is necessary to consider system constraints such as unknown and unmatched uncertainties.

1.3. Contribution

Most of the aforementioned approaches were designed with the assumption that the upper bound of the uncertainties is known. Hence, they suffered from pronounced chattering effects and singularity problems. To overcome these limitations, we propose in this paper an adaptive nonsingular integral-type SOSM approach. Its main contributions are as follows:

- A control design based on the second order SMC framework that employs an adaptation mechanism to estimate the bounds of the unknown uncertainty.
- An adaptation mechanism that enables synthesizing the controller without any assumption about the upper bound of the uncertainties; contrary to most existing approaches.
- A design that effectively attenuates the chattering effect and guarantees finite time convergence.

1.4. Paper organization

The paper is organized as follows: In Section 2, the considered class of nonlinear systems is introduced and the control problem is formulated. The main results including the integral type sliding surface design, the second order terminal sliding mode control methodology and the estimation-based control are discussed in Section 3. Simulation results illustrating the implementation of the proposed approach to a thruster system and an inverted pendulum are discussed in Section 4. Finally, some concluding remarks are reported in Section 5.

2. SYSTEM DESCRIPTION AND PRELIMINARIES

Consider the following uncertain nonlinear system:

$$\dot{x} = f(x) + g(x)u + w_u, \tag{1}$$

where $x \in R$ denotes the state vector, $u(t) \in R$ is the controller input, $f(x) \in R$ and $g(x) \in R$ is a known nonlinear functions with $g(x) \neq 0$, w_u represents the unmatched uncertainty satisfying $|w_u| \leq \Delta$, where Δ is a positive constant, and R denotes a set of real constant values.

The control objectives are to design a suitable controller u where the state trajectories x follow the reference signal $r \in R$ in the presence of unmatched uncertainties. The reference signal r is a differentiable function of time. Hence, the tracking error vector is formed by

$$e = x - r. \tag{2}$$

To meet the design specifications, we propose a nonsingular second order terminal sliding mode tracking control based on a rapid reaching law and an adaptation mechanism.

Assumption 1: The uncertainty term (w_u) does not guarantee the matched criterion i.e. it is not in the range space of controller.

Assumption 2: The unmatched uncertainty w_u is supposed to be bounded.

Definition 1 [36]**:** A time-invariant nonlinear system which is considered as

$$\dot{x}(t) = f(x), \tag{3}$$

so that $f(x) : D \to R^n$ is a vector function which is continuous and defined on an open vicinity D of equilibrium point. If the following conditions are satisfied, it can be said that the equilibrium point is entitled locally finite-time stable.

(I) The asymptotical stability in the subset $\hat{D} \subseteq D$ should be proved.

(II) The system should converge in $\hat{D}$ at the finite-time. Therefore, a convergence time $t_1(x_0)$ exists such that $x(t,x_0) \to 0$ as $t \to t_1(x_0)$and stays zero thereafter. Furthermore, if $\hat{D} = R^n$, the equilibrium point is globally finite-time stable.

Definition 2 [36]**:** Consider the following time-invariant affine nonlinear system:

$$\dot{x}(t) = f(x) + g(x)u(t), \tag{4}$$

so that $x(t) \in R^n$ specifies the state vector, $u(t) \in R^n$ denotes the control input, $f(0) = 0$ and $g(x) \neq 0$. If the equilibrium point of the affine system (4) using this controller becomes finite-time stable then the feedback control $u(t) = \Pi(x,t)$ is addressed as a finite-time stabilizing control law.

Lemma 1 [37]**:** Let $x \in \aleph \subset R^n$, $\dot{x} = \Im(x)$, $\Im : R^n \to R^n$ is a continuous function on an open vicinity $\aleph$ of zero and locally Lipschitz on $\aleph \setminus \{0\}$ and $\Im(0) = 0$. Assume there is a continuous function $V : \aleph \to R$ so that (a) the function V is positive-definite; (b) the time-derivative of V is negative on $\aleph \setminus \{0\}$; (c) there exist real positive scalars m and $0 < \alpha < 1$, and a vicinity $N \subset \aleph$ of the zero so that $\dot{V} + mV^{\alpha} \leq 0$ on $N \setminus \{0\}$. Thus, the zero is a finite-time stable equilibrium of $\dot{x} = \Im(x)$.

Thus, for each initial time t_0, the Lyapunov function converges to the origin in the finite time defined by

$$t_s = \frac{V(t_0)^{1-\alpha}}{m(1-\alpha)}, \tag{5}$$

where t_s is the settling time.

Definition 3: The sliding surface $s(t)$ is from order r if

$$s(t) = \dot{s}(t) = \ddot{s}(t) = \cdots = s(t)^{(r-1)} = 0. \tag{6}$$

3. DESIGN METHODOLOGY

3.1. Integral-type sliding surface

To ensure finite time tracking convergence, we consider the integral-type terminal sliding surface defined by

$$s = k_p e(t) + k_i \int_0^t e(\tau)^{q/p} d\tau + k_d \dot{e}, \tag{7}$$

where k_p, k_i, k_d are positive constants, and q and p are two odd positive integers with $q < p$. If the initial error e_0 is equal to zero, then the problem of tracking can be supposed as error on the sliding surface $s(t) = 0$ for all $t \geq 0$. If the system trajectory can arrive the surface $s(t) = 0$, it remains on it while sliding to $e(t) = 0$ and $\dot{e}(t) = 0$.

Once the tracking errors reach the terminal sliding surface $s = 0$, one obtains

$$k_p e(t) + k_i \int_0^t e(\tau)^{q/p} d\tau + k_d \dot{e} = 0, \tag{8}$$

and also $\dot{s} = 0$ is resulted, which produces

$$\ddot{e} = -\frac{k_p}{k_d}\dot{e} - \frac{k_i}{k_d} e^{q/p}. \tag{9}$$

Constructing the positive-definite Lyapunov function as

$$V_0 = 0.5\dot{e}^2 + \frac{k_i p}{k_d(q+p)} e^{1+q/p}. \tag{10}$$

Differentiating V_0 and using (9) yields

$$\begin{aligned} \dot{V}_0 =& \dot{e}\ddot{e} + \frac{k_i p}{k_d (q+p)} \left(\frac{q}{p} + 1\right) e^{q/p}\dot{e} \\ =& \dot{e}\left(-\frac{k_p}{k_d}\dot{e} - \frac{k_i}{k_d} e^{q/p}\right) + \frac{k_i}{k_d} e^{q/p}\dot{e} \\ =& -\frac{k_p}{k_d}\dot{e}^2 \leq 0. \end{aligned} \tag{11}$$

The above equation shows that once the trajectory of error reaches the sliding surface (7), the error signal converges to the origin asymptotically. Actually, the error state is uniformly bounded. Since the function V_0 is positive-definite and its time derivative is negative semi-definite, it results that $\lim_{t\to\infty} V_0 = V_0(\infty)$ exists for $V_0(\infty) \in R^+$. According to the boundedness of the error signal, $\dot{V}_0$ is uniformly continuous. Thus, using Barbalat lemma, it can be found that $\lim_{t\to\infty} \dot{e}(t) = 0$. One can obtain from (7) that $\lim_{t\to\infty} e(t) = 0$. Finally, the error signal converges to zero asymptotically.

3.2. Second-order terminal sliding model control

In this part, an integral-type second-order sliding surface associated with the terminal sliding mode control approach is designed. In the second-order sliding mode control, the aim of control is to drive s and $\dot{s}$ to the origin, i.e., $s = \dot{s} = 0$. The integral-type second-order terminal sliding surface is defined by

$$\dot{s} + bs = k_p e + k_i \int_0^t e(\tau)^{q/p} d\tau + k_d \dot{e}, \tag{12}$$

where b indicates a positive coefficient which governs the decline rate of s. Taking the time-derivative of (12), one finds

$$\ddot{s} + b\dot{s} = k_p \dot{e} + k_i e^{q/p} + k_d \ddot{e}. \tag{13}$$

A necessary condition for the error state to stay on the switching surface is $\dot{s} = \ddot{s} = 0$. Hence, the characteristic polynomial (9) is achieved.

The first and second-order derivatives of error signal (2) are found as

$$\dot{e} = f(x) + g(x)u + w_u - \dot{r}, \tag{14}$$

$$\ddot{e} = \dot{f}(x) + \dot{g}(x)u + g(x)\dot{u} + \dot{w}_u - \ddot{r}. \tag{15}$$

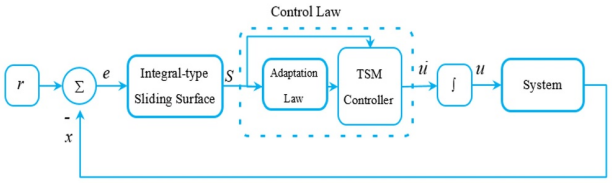

Fig. 1. The schematic view of the proposed controller.

Substituting (14) and (15) in (13), yields

$$\begin{aligned}\ddot{s}+b\dot{s} =&k_p(f(x)+g(x)u+w_u-\dot{r})+k_i e^{q/p}\\ &+k_d(\dot{f}(x)+\dot{g}(x)u+\dot{w}_u-\ddot{r})+k_d g(x)\dot{u}.\end{aligned} \tag{16}$$

The signal of equivalent control is achieved from the above equation when $\ddot{s}=0$. It is a necessary criterion to guarantee the error states reach the switching surface. The equivalent controller is found as

$$\begin{aligned}\dot{u}_{eq} =&(k_d g(x))^{-1}(b\dot{s}-k_p(f(x)+g(x)u_{eq}-\dot{r})\\ &-k_i e^{q/p}-k_d(\dot{f}(x)+\dot{g}(x)u_{eq}-\ddot{r})\Big).\end{aligned} \tag{17}$$

The switching controller is designed as

$$\begin{aligned}\dot{u}_S =&-(k_d g(x))^{-1}((k_p g(x)+k_d\dot{g}(x))u_S\\ &+m_1|\dot{s}|sgn(\dot{s})+\delta sgn(\dot{s})+m_2|\dot{s}|^{\alpha}sgn(\dot{s})),\end{aligned} \tag{18}$$

where $m_1, m_2>0$, $0<\alpha<1$, $\delta\geq|s|+|k_p w_u+k_d\dot{w}_u|$. In the switching control law $\dot{u}_S$ (18), the discontinuous sign function ($sgn(\dot{s})$) operates on first time-derivative of control law. After integration, the obtained controller is continuous and chattering free. The schematic diagram of the proposed controller is illustrated in Fig. 1.

Theorem 1: Consider the uncertain nonlinear system (1) and integral-type switching surface (7). Using (17) and (18), the total control signal is defined as

$$\begin{aligned}\dot{u} =&-(k_d g(x))^{-1}\{k_p(f(x)+g(x)u_{eq}-\dot{r})-b\dot{s}\\ &+k_i e^{q/p}+k_d(\dot{f}(x)+\dot{g}(x)u_{eq}-\ddot{r})\\ &+(k_p g(x)+k_d\dot{g}(x))u_S+m_1|\dot{s}|sgn(\dot{s})\\ &+m_2|\dot{s}|^{\alpha}sgn(\dot{s})+\delta sgn(\dot{s})\},\end{aligned} \tag{19}$$

where $\delta\geq|s|+|k_p w_u+k_d\dot{w}_u|$. Then, the integral-type sliding surface s and time-derivative of sliding surface $\dot{s}$ are forced to converge to the equilibrium.

Proof: If (17)-(18) are substituted in (16), we have

$$\begin{aligned}\ddot{s} =&k_p w_u+k_d\dot{w}_u-\delta sgn(\dot{s})\\ &-m_1|\dot{s}|sgn(\dot{s})-m_2|\dot{s}|^{\alpha}sgn(\dot{s}).\end{aligned} \tag{20}$$

Considering the candidate Lyapunov function:

$$V_1=0.5\left(s^2+\dot{s}^2\right). \tag{21}$$

Differentiating (21) and using (20), one obtains

$$\begin{aligned}\dot{V}_1 =&s\dot{s}+\dot{s}\ddot{s}\\ =&s\dot{s}+\dot{s}[k_p w_u+k_d\dot{w}_u-\delta sgn(\dot{s})\\ &-m_1|\dot{s}|sgn(\dot{s})-m_2|\dot{s}|^{\alpha}sgn(\dot{s})]\\ \leq&(|s|+|k_p w_u+k_d\dot{w}_u|-\delta)|\dot{s}|-m_1|\dot{s}|^2-m_2|\dot{s}|^{\alpha+1}\\ \leq&-m_1|\dot{s}|^2-m_2|\dot{s}|^{\alpha+1}<0.\end{aligned} \tag{22}$$

Since the time-derivative of Lyapunov function is negative definite, then, the Lyapunov function (21) decreases gradually and the switching surface $s(t)$ and its time-derivative converge to origin. □

3.3. Estimation-based control

It is practically difficult to find the upper bound of the uncertainty terms w_u and $\dot{w}_u$. Hence, an estimation parameter $\hat{\delta}$ is required to be designed. In the subsequent theorem, an adaptive approach is presented to estimate the unknown uncertainty bound.

Theorem 2: Consider the uncertain nonlinear system (1) and integral-type terminal sliding surface (7). Suppose that the uncertainty terms w_u and $\dot{w}_u$ are bounded, but the upper bound of uncertainties is unknown. Then, using the parameter-tuning terminal sliding tracking controller

$$\begin{aligned}\dot{u} =&-(k_d g(x))^{-1}\{k_p(f(x)+g(x)u_{eq}-\dot{r})-b\dot{s}\\ &+k_i e^{q/p}+k_d(\dot{f}(x)+\dot{g}(x)u_{eq}-\ddot{r})\\ &+(k_p g(x)+k_d\dot{g}(x))u_S+m_1|\dot{s}|sgn(\dot{s})\\ &+m_2|\dot{s}|^{\alpha}sgn(\dot{s})+\hat{\delta}sgn(\dot{s})\},\end{aligned} \tag{23}$$

with $\hat{\delta}$ as the estimated variable of δ, and adaptation law as

$$\dot{\hat{\delta}}=\ell^{-1}|\dot{s}|, \tag{24}$$

with $\ell>0$, the reachability criterion of the sliding surface is fulfilled and the terms s and $\dot{s}$ converge to zero.

Proof: Consider the estimation error as

$$\tilde{\delta}=\hat{\delta}-\delta, \tag{25}$$

where differentiating $\tilde{\delta}$ and using (24), one has

$$\dot{\tilde{\delta}}=\ell^{-1}|\dot{s}|. \tag{26}$$

Substituting the adaptive terminal sliding tracker (23) into (16), one obtains

$$\begin{aligned}\ddot{s} =&k_p w_u+k_d\dot{w}_u-\hat{\delta}sgn(\dot{s})\\ &-m_1|\dot{s}|sgn(\dot{s})-m_2|\dot{s}|^{\alpha}sgn(\dot{s}).\end{aligned} \tag{27}$$

The Lyapunov function is considered as

$$\dot{V}_2=0.5\left(s^2+\dot{s}^2+\ell\tilde{\delta}^2\right). \tag{28}$$

Taking the time-derivative of (28) yields

$$\begin{aligned}\dot{V}_2 =& s\dot{s}+\dot{s}\ddot{s}+\ell\tilde{\delta}\dot{\tilde{\delta}}\\ =&(s+\ddot{s})\dot{s}+(\hat{\delta}-\delta)|\dot{s}|.\end{aligned} \tag{29}$$

Now, using (27) and (29), one achieves

$$\begin{aligned}\dot{V}_2 =&(k_p w_u+k_d\dot{w}_u-\hat{\delta}sgn(\dot{s})-m_1|\dot{s}|sgn(\dot{s})\\ &-m_2|\dot{s}|^{\alpha}sgn(\dot{s})+s)\dot{s}+(\hat{\delta}-\delta)|\dot{s}|\\ =&(k_p w_u+k_d\dot{w}_u)\dot{s}-\hat{\delta}|\dot{s}|-m_1|\dot{s}|^2\\ &-m_2|\dot{s}|^{\alpha+1}+s\dot{s}+(\hat{\delta}-\delta)|\dot{s}|.\end{aligned} \tag{30}$$

Since $s\leq|s|$ and $(k_p w_u+k_d\dot{w}_u)\dot{s}\leq|k_p w_u+k_d\dot{w}_u||\dot{s}|$, (30) is written as

$$\begin{aligned}\dot{V}_2 \leq&\left(|k_p w_u+k_d\dot{w}_u|+|s|-\hat{\delta}\right)|\dot{s}|-m_1|\dot{s}|^2-m_2|\dot{s}|^{\alpha+1}\\ &+(\hat{\delta}-\delta)|\dot{s}|.\end{aligned} \tag{31}$$

Addition and subtraction of term $\delta|\dot{s}|$ to (31), yields

$$\begin{aligned}\dot{V}_2 \leq&\left(|k_p w_u+k_d\dot{w}_u|+|s|-\hat{\delta}\right)|\dot{s}|-m_1|\dot{s}|^2-m_2|\dot{s}|^{\alpha+1}\\ &+(\hat{\delta}-\delta)|\dot{s}|+\delta|\dot{s}|-\delta|\dot{s}|\\ =&-\left(\delta-|k_p w_u+k_d\dot{w}_u|-|s|\right)|\dot{s}|-m_1|\dot{s}|^2-m_2|\dot{s}|^{\alpha+1}\\ &-\hat{\delta}|\dot{s}|+\hat{\delta}|\dot{s}|+\delta|\dot{s}|-\delta|\dot{s}|\\ \leq&-m_1|\dot{s}|^2-m_2|\dot{s}|^{\alpha+1}<0.\end{aligned} \tag{32}$$

Hence, due to the parameter-tuning terminal sliding tracker (23), it is resulted that the Lyapunov function (28) reduces gradually and the reachability criterion of the sliding surface is satisfied. This finishes the proof. □

4. SIMULATION RESULTS

The effectiveness of the proposed approach is illustrated using two illustrative examples: a thruster system and an inverted pendulum. The obtained results are detailed below.

4.1. Example 1: Thruster system

Consider the thruster system depicted in Fig. 2 [38]. Its dynamics are modeled by [38]

$$\dot{\Omega}=\beta\tau-\varepsilon|\Omega|\Omega, \tag{33}$$

where Ω is the propeller's angular velocity, τ is the input torque, ε and β are dynamic constants which are 0.037 and 42 $1/(vs^2)$. By considering $r=\sin(t)$ as the reference function, the state tracking error is $e=\Omega-r$. Formulating the sliding surface using (7) and deriving the control input yields:

$$\begin{aligned}\dot{u}=&\dot{\tau}=-(k_d\beta)^{-1}(k_p(-\varepsilon|\Omega|\Omega+\beta\tau_{eq}-\cos t)-b\dot{s}\\ &+k_i e^{q/p}+k_d(-\varepsilon\frac{\Omega^2}{|\Omega|}-\varepsilon|\Omega|+\sin t)+k_p\beta\tau_S\\ &+m_1|\dot{s}|sgn(\dot{s})+m_2|\dot{s}|^{\alpha}sgn(\dot{s})+\delta sgn(\dot{s})),\end{aligned} \tag{34}$$

where the equivalent and switching control laws are obtained from the following equations:

$$\begin{aligned}\dot{u}_{eq}=\dot{\tau}_{eq}=&(k_d\beta)^{-1}\Big(b\dot{s}-k_p(-\varepsilon|\Omega|\Omega+\beta\tau_{eq}\\ &-\cos t)-k_i e^{q/p}-k_d(-\varepsilon\frac{\Omega^2}{|\Omega|}-\varepsilon|\Omega|+\sin t)\Big),\end{aligned} \tag{35}$$

$$\begin{aligned}\dot{u}_S=\dot{\tau}_S=&-(k_d\beta)^{-1}(k_p\beta\tau_S+m_1|\dot{s}|sgn(\dot{s})\\ &+m_2|\dot{s}|^{\alpha}sgn(\dot{s})+\delta sgn(\dot{s})).\end{aligned} \tag{36}$$

The constant parameters of the system are illustrated in Table 1. The design parameters are determined by trial and error method.

Table 1. Constant parameters.

Parameter	Value	Parameter	Value
A	0.9	m_1	10
k_d	0.004	m_2	0.1
k_p	9	b	10
k_i	4	l	0.0025
α	0.9	δ	0.01
p	3	q	5

By applying (34) to the thruster system (33), the following figures are obtained. Figs. 1-4 represent the state variable trajectory, control signal, sliding surface and trajectory error, respectively. All of these simulation results are compared with the adaptive super-twisting TSMC method which is presented in [35]. Fig. 3 illustrates that the state tracks sine function well. The proposed method has smoother response than the method of [39]. Fig. 4 represents the controller input plot. The torque of system does not have notable overshoot and with appropriate amplitude, it can control thruster system. However, the method of [39] has chattering and higher amplitude, and this behavior may damage the system. Fig. 5 displays that the

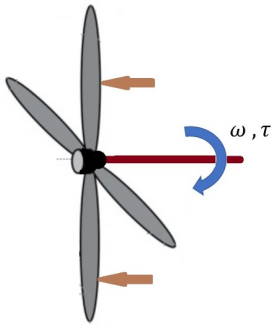

Fig. 2. The thruster schematic system.

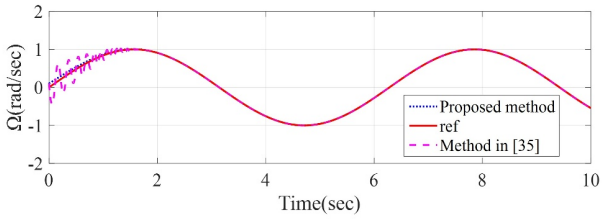

(a)

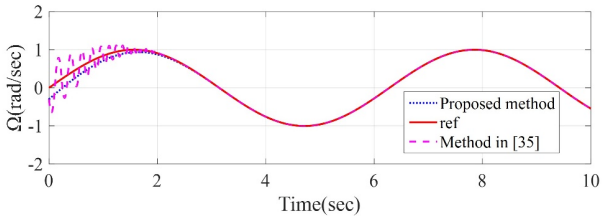

(b)

Fig. 3. State trajectory Ω for (a) initial value of 0.1 (rad/sec), (b) initial value of 0.5 (rad/sec).

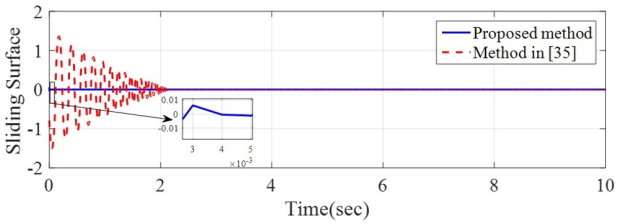

(a)

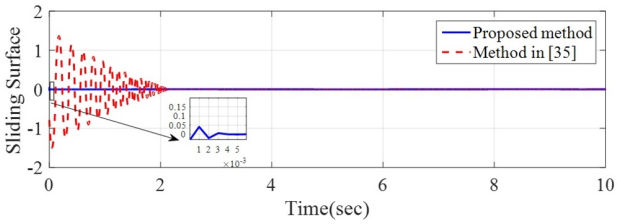

(b)

Fig. 5. Sliding surface for (a) initial value of 0.1 (rad/sec), (b) initial value of 0.5 (rad/sec).

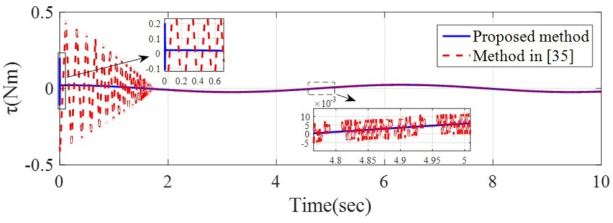

(a)

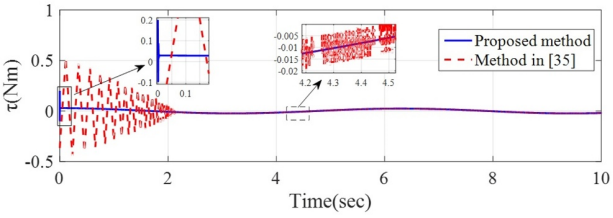

(b)

Fig. 4. Control signal τ for (a) initial value of 0.1 (rad/sec), (b) initial value of 0.5 (rad/sec).

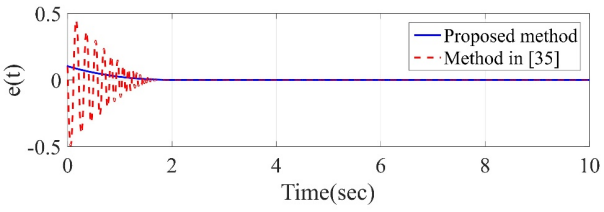

(a)

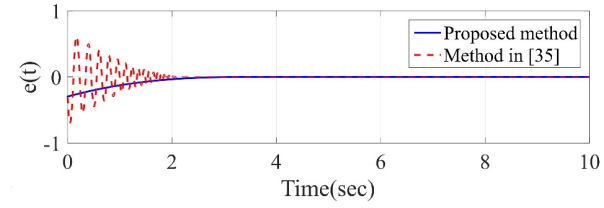

(b)

Fig. 6. Errors of state trajectories for (a) initial value of 0.1 (rad/sec), (b) initial value of 0.5 (rad/sec).

sliding surface of the suggested method converges to zero without chattering. Fig. 6 illustrates that the error of state trajectory converges to origin. Therefore, the closed-loop system is stabilized, trajectory task is done well and efficiency and accuracy of suggested method is significant. The changes of initial values indicate the robustness of proposed method.

4.2. Example2: Inverted pendulum

To demonstrate the efficiency of the proposed approach, we implement it to the inverted pendulum, depicted in

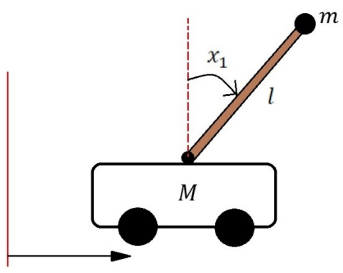

Fig. 7. Inverted pendulum schematic.

Fig. 7, which dynamics are modeled by [40]

$$\begin{aligned}\dot{x}_1 &= x_2,\\ \dot{x}_2 &= \frac{g\sin(x_1) - aml x_2^2\sin(2x_2)/2 - a\cos(x_1)u}{4l/3 - aml\cos^2(x_1)} + w,\end{aligned} \tag{37}$$

where x_1 is the pendulum angle from vertical, x_2 is the angular velocity, g denotes the gravity constant, $2l$ represents the length of pendulum, $a = 1/(m+M)$ where m is the mass of pendulum, $M$is the mass of the cart, and $w(t) = 0.01\sin(t)$ represents the external disturbance.

The reference inputs are $0.5\sin(t)$, for the first state trajectory and $0.5\cos(t)$ for the second state. Considering the sliding surface (7), and designing the controller according to the approach detailed in 3 yields the following control law:

$$\begin{aligned}\dot{u} = &-(k_d\frac{a\cos(x_1)}{4l/3 - aml\cos^2(x_1)})^{-1}\\ &\times(k_p(\frac{g\sin(x_1) - aml x_2^2\sin(2x_2)/2}{4l/3 - aml\cos^2(x_1)} - 0.5\cos t\\ &+\frac{a\cos(x_1)}{4l/3 - aml\cos^2(x_1)}u_{eq}) - b\dot{s} + k_i e_2{}^{q/p}\\ &+k_d(\frac{d}{dt}\left(\frac{g\sin(x_1) - aml x_2^2\sin(2x_2)/2}{4l/3 - aml\cos^2(x_1)}\right)\\ &+\frac{d}{dt}\left(\frac{a\cos(x_1)}{4l/3 - aml\cos^2(x_1)}\right)u_{eq} + 0.5\sin t)\\ &+k_p(\frac{a\cos(x_1)}{4l/3 - aml\cos^2(x_1)}\\ &+\frac{d}{dt}\left(\frac{g\sin(x_1) - aml x_2^2\sin(2x_2)/2}{4l/3 - aml\cos^2(x_1)}\right))u_S\\ &+m_1|\dot{s}|sgn(\dot{s}) + m_2|\dot{s}|^{\alpha}sgn(\dot{s}) + \delta sgn(\dot{s})),\end{aligned} \tag{38}$$

where u_{eq} and u_S are obtained from the following equations:

$$\begin{aligned}\dot{u}_{eq} = &\frac{4l/3 - aml\cos^2(x_1)}{ak_d\cos(x_1)}\\ &\times(-k_p(\frac{g\sin(x_1) - aml x_2^2\sin(2x_2)/2}{4l/3 - aml\cos^2(x_1)}\\ &+\frac{a\cos(x_1)}{4l/3 - aml\cos^2(x_1)}u_{eq} - 0.5\cos t)\\ &-k_i e_2{}^{q/p} + b\dot{s}\\ &-k_d(\frac{d}{dt}\left(\frac{g\sin(x_1) - aml x_2^2\sin(2x_2)/2}{4l/3 - aml\cos^2(x_1)}\right)\\ &+\frac{d}{dt}\left(-\frac{a\cos(x_1)}{4l/3 - aml\cos^2(x_1)}\right)u_{eq} + 0.5\sin t)),\end{aligned} \tag{39}$$

$$\begin{aligned}\dot{u}_S = &-(k_d\frac{a\cos(x_1)}{4l/3 - aml\cos^2(x_1)})^{-1}\\ &\times(k_p(\frac{a\cos(x_1)}{4l/3 - aml\cos^2(x_1)}\\ &+\frac{d}{dt}\left(\frac{g\sin(x_1) - aml x_2^2\sin(2x_2)/2}{4l/3 - aml\cos^2(x_1)}\right))u_S\\ &+m_1|\dot{s}|sgn(\dot{s}) + m_2|\dot{s}|^{\alpha}sgn(\dot{s}) + \delta sgn(\dot{s})),\end{aligned} \tag{40}$$

Table 2. Constant parameters.

Parameter	Value	Parameter	Value
a	0.01	m_1	0.01
k_d	0.2	m_2	0.1
k_p	1.5	b	0.845
k_i	1.9	l	0.01
α	0.01	δ	0.02
p	3	q	5

The system parameters are illustrated in Table 2. The design parameters of the system are found by trial and error.

Applying (38) to the inverted pendulum system (37), yields the simulation results depicted in Figures 9 through 13. Note that two initial values were considered in the figures to illustrate the robustness of the proposed controller.

Figs. 5-9 show the dynamics of the angular velocity, the controller law, the sliding surface and the trajectory error, respectively. Fig. 8 shows that the first state $(x_1(t))$ tracks the reference well for two distinct initial values. Note that though convergence time is more than that of the method in [39],the error converges to zero after 1.5 seconds, whereas the error value of [39] is more than the suggested method sometimes. Fig. 9 depicts the state $x_2(t)$ trajectory of the reference function. It is clear that the tracking performance of the suggested method for $x_2(t)$ is better than the results of the method of [39]. Fig. 10 depicts the bounded control signal. The control signal amplitude of the proposed method is very small compared to the method in [39] for both initial values. Fig. 11 clearly shows that the sliding surface of the proposed method converges to zero without chattering. Figs. 12 and 13 depict that the error of the state trajectory converges to the origin whereas in [39], we cannot assert that the error is exactly zero.

Based on the above results, we can conclude that the proposed control stabilized the systems and achieved good tracking performance, whilst attenuating chattering.

Remark 1: The design parameters are to be selected such that a compromise between tracking accuracy, control signal amplitude and convergence speed is obtained. This can be achieved by considering some observations as follows:

The increase of the parameters k_p, k_i and k_d causes the improvement of the tracking accuracy, enhancement of convergence speed and increment of the control signal amplitude.

The increase of the parameters δ and α makes the improvement of the convergence rate and tracking accuracy;

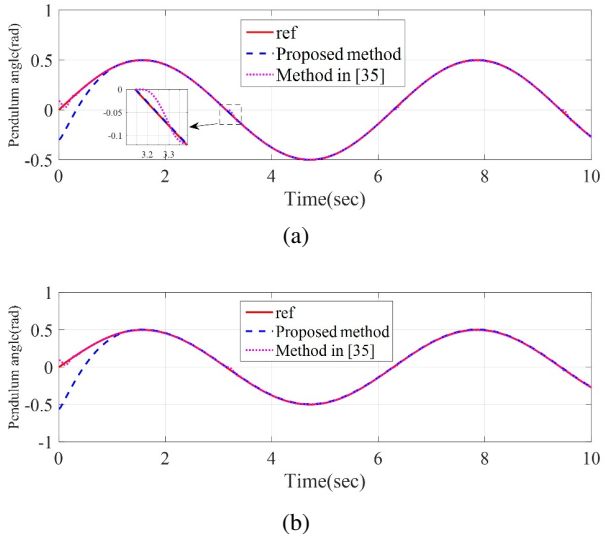

Fig. 8. tate trajectory $x_1(t)$ for (a) initial value of -0.1 (rad/sec), (b) initial value of 0.3 (rad/sec).

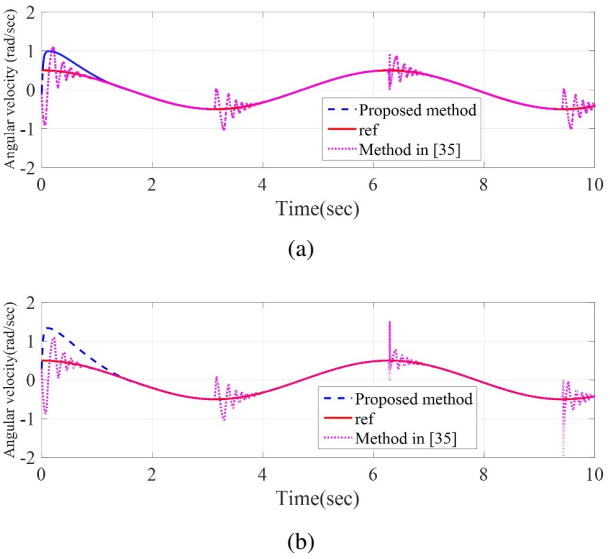

Fig. 9. State trajectory $x_2(t)$ for (a) initial value of -0.1 (rad/sec), (b) initial value of 0.3 (rad/sec).

however, it causes increase of the controller amplitude and observation of chattering problem in the control signals.

5. CONCLUSION

This paper proposed a novel adaptive nonsingular integral-type second-order terminal sliding mode tracking controller for a class of nonlinear systems with uncertainties. Contrary to existing approaches, the design does not rely on the assumption that the upper bound of the uncertainties is known, instead, it estimates the unknown uncertainty bound via an adaptive approach. The proposed

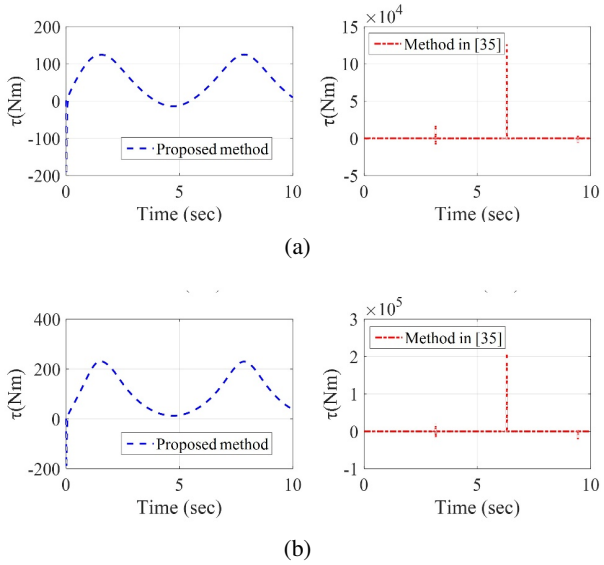

Fig. 10. Control signal for (a) initial value of -0.1 (rad/sec), (b) initial value of 0.3 (rad/sec).

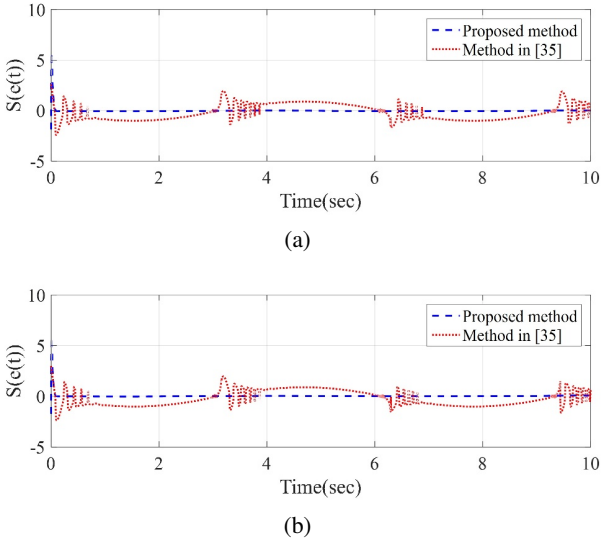

Fig. 11. FTSM surface $s(e(t))$ for (a) initial value of -0.1 (rad/sec), (b) initial value of 0.3 (rad/sec).

approach was validated using a thruster system and an inverted pendulum. The stability of the closed loop system was proven using the Lyapunov theory. In addition to eliminating the need for the knowledge of the upper bound limit, the proposed approach ensured finite time stability and properly mitigated external disturbances, whilst attenuating the chattering effect. Generalizing the proposed approach to encompass high-order systems with input saturation and time-varying delays will be the focus of our future works.

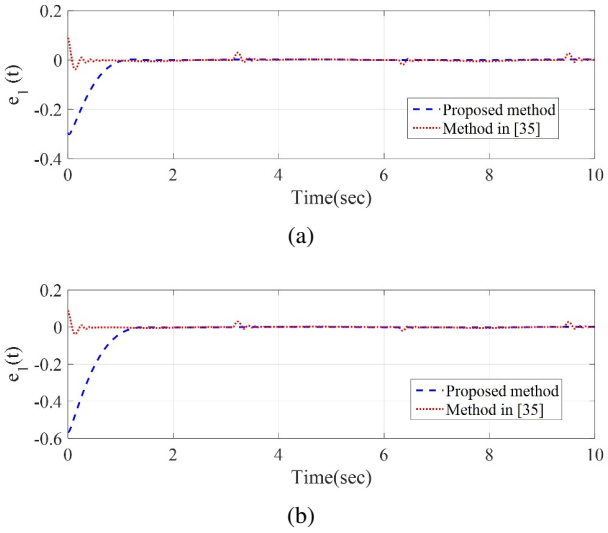

Fig. 12. Trajectory error $e_1(t)$ for (a) initial value of -0.1 (rad/sec), (b) initial value of 0.3 (rad/sec).

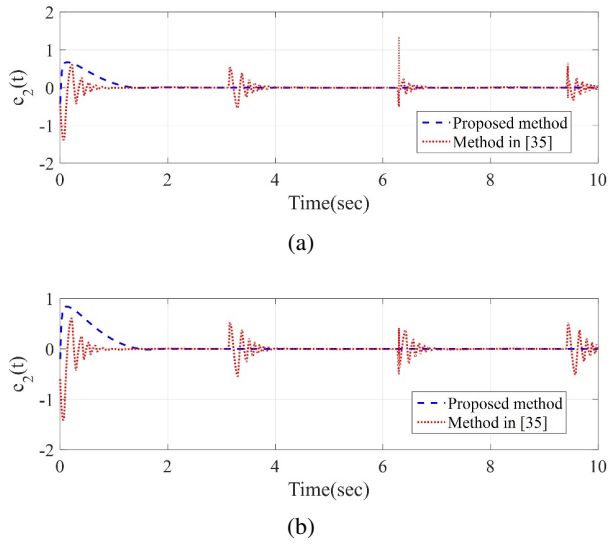

Fig. 13. Trajectory error $e_2(t)$ for (a) initial value of -0.1 (rad/sec), (b) initial value of 0.3 (rad/sec).

REFERENCES

[1] Y. Wei, H. Yu, H. R. Karimi, and Y. H. Joo, "New approach to fixed-order output-feedback control for piecewise-affine systems," *IEEE Transactions on Circuits and Systems I: Regular Papers*, vol. 65, pp. 2961-2969, 2018.

[2] Y. Wei, J. H. Park, J. Qiu, L. Wu, and H. Y. Jung, "Sliding mode control for semi-Markovian jump systems via output feedback," *Automatica*, vol. 81, pp. 133-141, 2017.

[3] S. S. Parker, J. Krantz, E.-A. Kwak, N. K. Barker, C. G. Deer, N. Y. Lee, G. Mouneimne, and P. R. Langlais, "Insulin induces microtubule stabilization and regulates the microtubule plus-end tracking protein network in adipocytes," *Molecular & Cellular Proteomics*, vol. 18, pp. 1363-1381, 2019.

[4] J. Luo, Z. Yin, C. Wei, and J. Yuan, "Low-complexity prescribed performance control for spacecraft attitude stabilization and tracking," *Aerospace Science and Technology*, vol. 74, pp. 173-183, 2018.

[5] X. Liu, S. Qi, R. Malekain, and Z. Li, "Observer-based composite adaptive dynamic terminal sliding-mode controller for nonlinear uncertain SISO systems," *International Journal of Control, Automation and Systems*, vol. 17, pp. 94-106, 2019.

[6] J. Kumar, V. Kumar, and K. Rana, "Design of robust fractional order fuzzy sliding mode PID controller for two link robotic manipulator system," *Journal of Intelligent & Fuzzy Systems*, vol. 35, pp. 5301-5315, 2018.

[7] W. Sun, Y. Wu, and L. Wang, "Trajectory tracking of constrained robotic systems via a hybrid control strategy," *Neurocomputing*, vol. 330, pp. 188-195, 2019.

[8] H. Li, P. Shi, D. Yao, and L. Wu, "Observer-based adaptive sliding mode control for nonlinear Markovian jump systems," *Automatica*, vol. 64, pp. 133-142, 2016.

[9] Q. Liu, R. Li, Q. Zhang, and J. Li, "Adaptive robust H∞ sliding mode control for singular systems with time-varying delay and uncertain derivative matrix," *International Journal of Control, Automation and Systems*, vol. 17, no. 7, pp. 3179-3193, 2019.

[10] B. Jiang, H. R. Karimi, S. Yang, C. Gao, and Y. Kao, "Observer-based adaptive sliding mode control for nonlinear stochastic Markov jump systems via TS fuzzy modeling: Applications to robot arm model," *IEEE Transactions on Industrial Electronics*, 2020. DOI: 10.1109/TIE.2020.2965501

[11] Z. Liu, H. R. Karimi, and J. Yu, "Passivity-based robust sliding mode synthesis for uncertain delayed stochastic systems via state observer," *Automatica*, vol. 111, p. 108596, 2020.

[12] H. Karami and R. Ghasemi, "Fixed time terminal sliding mode trajectory tracking design for a class of nonlinear dynamical model of air cushion vehicle," *SN Applied Sciences*, vol. 2, p. 98, 2020.

[13] A. Levant and L. Alelishvili, "Integral high-order sliding modes," *IEEE Transactions on Automatic control*, vol. 52, pp. 1278-1282, 2007.

[14] T. Elmokadem, M. Zribi, and K. Youcef-Toumi, "Terminal sliding mode control for the trajectory tracking of underactuated autonomous underwater vehicles," *Ocean Engineering*, vol. 129, pp. 613-625, 2017.

[15] L. Tao, Q. Chen, Y. Nan, and C. Wu, "Double hyperbolic reaching law with chattering-free and fast convergence," *IEEE Access*, vol. 6, pp. 27717-27725, 2018.

[16] N. B. Cheng, L. W. Guan, L. P. Wang, and J. Han, "Chattering reduction of sliding mode control by adopting nonlinear saturation function," *Advanced Materials Research*, pp. 53-61, 2011.

[17] M. Mihoub, A. S. Nouri, and R. B. Abdennour, "Real-time application of discrete second order sliding mode control to a chemical reactor," *Control Engineering Practice*, vol. 17, pp. 1089-1095, 2009.

[18] G. Bartolini, A. Ferrara, and E. Usai, "Chattering avoidance by second-order sliding mode control," *IEEE Transactions on automatic control*, vol. 43, pp. 241-246, 1998.

[19] W.-C. Su, S. V. Drakunov, and U. Ozguner, "An O (T/sup 2/) boundary layer in sliding mode for sampled-data systems," *IEEE Transactions on Automatic Control*, vol. 45, pp. 482-485, 2000.

[20] S. Liu, Y. Liu, and N. Wang, "Nonlinear disturbance observer-based backstepping finite-time sliding mode tracking control of underwater vehicles with system uncertainties and external disturbances," *Nonlinear Dynamics*, vol. 88, pp. 465-476, 2017.

[21] A. Levant, "Chattering analysis," *IEEE Transactions on Automatic Control*, vol. 55, pp. 1380-1389, 2010.

[22] Y. Feng, X. Yu, and F. Han, "On nonsingular terminal sliding-mode control of nonlinear systems," *Automatica*, vol. 49, pp. 1715-1722, 2013.

[23] A. Goel and A. Swarup, "Chattering free trajectory tracking control of a robotic manipulator using high order sliding mode," *Advances in Computer and Computational Sciences*, ed: Springer, pp. 753-761, 2017.

[24] G. Bartolini, A. Pisano, and E. Usai, "Second-order sliding-mode control of container cranes," *Automatica*, vol. 38, pp. 1783-1790, 2002.

[25] H. Joe, M. Kim, and S. Yu, "Second-order sliding-mode controller for autonomous underwater vehicle in the presence of unknown disturbances," *Nonlinear Dynamics*, vol. 78, pp. 183-196, 2014.

[26] Q. Meng, C. Qian, and R. Liu, "Dual-rate sampled-data stabilization for active suspension system of electric vehicle," *International Journal of Robust and Nonlinear Control*, vol. 28, pp. 1610-1623, 2018.

[27] H. Shen, F. Li, H. Yan, H. R. Karimi, and H.-K. Lam, "Finite-time event-triggered $\mathcal{H}_\infty$ control for T–S fuzzy Markov jump systems," *IEEE Transactions on Fuzzy Systems*, vol. 26, pp. 3122-3135, 2018.

[28] Y. H. Joo and P. X. Duong, "Adaptive neural network second-order sliding mode control of dual arm robots," *International Journal of Control, Automation and Systems*, vol. 15, pp. 2883-2891, 2017.

[29] A. Swikir and V. Utkin, "Chattering analysis of conventional and super twisting sliding mode control algorithm," *Proc. of 14th International Workshop on Variable Structure Systems (VSS)*, pp. 98-102, 2016.

[30] Y. Yang, "A time-specified nonsingular terminal sliding mode control approach for trajectory tracking of robotic airships," *Nonlinear Dynamics*, vol. 92, pp. 1359-1367, 2018.

[31] G. P. Incremona, M. Cucuzzella, and A. Ferrara, "Second order sliding mode control for nonlinear affine systems with quantized uncertainty," *Automatica*, vol. 86, pp. 46-52, 2017.

[32] G. P. Incremona, M. Cucuzzella, and A. Ferrara, "Adaptive suboptimal second-order sliding mode control for microgrids," *International Journal of Control*, vol. 89, pp. 1849-1867, 2016.

[33] S. Ding, J. H. Park, and C.-C. Chen, "Second-order sliding mode controller design with output constraint," *Automatica*, vol. 112, p. 108704, 2020.

[34] M. R. Amini, M. Shahbakhti, S. Pan, and J. K. Hedrick, "Discrete adaptive second order sliding mode controller design with application to automotive control systems with model uncertainties," *Proc. of American Control Conference (ACC)*, pp. 4766-4771, 2017.

[35] A. Pisano, M. Tanelli, and A. Ferrara, "Switched/time-based adaptation for second-order sliding mode control," *Automatica*, vol. 64, pp. 126-132, 2016.

[36] S. P. Bhat and D. S. Bernstein, "Finite-time stability of continuous autonomous systems," *SIAM Journal on Control and Optimization*, vol. 38, pp. 751-766, 2000.

[37] C. Xiu and P. Guo, "Global terminal sliding mode control with the quick reaching law and its application," *IEEE Access*, vol. 6, pp. 49793-49800, 2018.

[38] D. R. Yoerger, J. G. Cooke, and J.-J. Slotine, "The influence of thruster dynamics on underwater vehicle behavior and their incorporation into control system design," *IEEE Journal of Oceanic Engineering*, vol. 15, pp. 167-178, 1990.

[39] M.-C. Pai, "Adaptive super-twisting terminal sliding mode control for nonlinear systems with multiple inputs," *International Journal of Dynamics and Control*, pp. 1-9, 2019.

[40] W. Ji, J. Qiu, L. Wu, and H.-K. Lam, "Fuzzy-affine-model-based output feedback dynamic sliding mode controller design of nonlinear systems," *IEEE Transactions on Systems, Man, and Cybernetics: Systems*, 2019. DOI: 10.1109/TSMC.2019.2900050

Saleh Mobayen received his Ph.D. in control engineering from Tarbiat Modares University, Tehran, Iran, in 2013. He is currently an Associate Professor with the Department of Electrical Engineering of University of Zanjan, Zanjan, Iran. He has published several papers in the national and international journals. He is a member of the Institute of Electrical and Electronics Engineers (IEEE), a member of the IEEE control systems society and serves as a member of program committee of several international conferences. Dr. Mobayen is the Associate Editor of Artificial Intelligence Review, Associate Editor of International Journal of Control, Automation and Systems, Associate Editor of Circuits, Systems, and Signal Processing, Associate Editor of Simulation, Associate Editor of Measurement and Control, Academic Editor of Complexity, Associate Editor of International Journal of Dynamics and Control, Academic Editor of Mathematical Problems in Engineering, Associate Editor of SN Applied Sciences, Editorial Board Member of International Journal of Modelling, Identification and Control, and Editorial Board Member of Journal of Electronic & Information Systems. His research interests include control theory, sliding mode control, robust tracking, non-holonomic robots and chaotic systems.

Hamede Karami was born in Kermanshah, Iran, in 1990. She was graduated in M.Sc. degree in control engineering in 2019 at the University of Qom, Iran and now she is a Ph.D. student in control engineering at the University of Zanjan, Zanjan, Iran. She has several papers in national and international conferences and journals. Her research interest includes nonlinear control and the application of sliding-mode control on mechanical and electromechanical systems.

Afef Fekih received her B.S., M.S., and Ph.D. degrees all in electrical engineering from the National Engineering School of Tunis, Tunisia, in 1995, 1998, and 2002, respectively. Currently, she is a Full Professor in the Department of Electrical and Computer Engineering and the Chevron/BORSF Professor in Engineering at University of Louisiana at Lafayette. Her research interests focus on control theory and applications, including nonlinear and robust control, optimal control, and fault tolerant control with applications to power systems, wind turbines, unmanned vehicles and automotive engines. Dr. Fekih is a senior member of the Institute of Electrical and Electronics Engineers (IEEE), a member of the IEEE control systems society, IEEE Power and Energy society and the IEEE women in Engineering society. She is the vice chair and media coordinator for the IEEE CSS Women in Control group (WiC), a member of the IEEE Technology conference editorial board and a member of the AACC & CSS TC on Control Education. She has served as a reviewer and guest editor for numerous journals and conferences.